A Class of Airfoils Designed for High Lift in Incompressible Flow

Robert H. Liebeck*
Douglas Aircraft Company, McDonnell Douglas Corporation, Long Beach, Calif.

The problem studied is that of designing a single element airfoil which provides the maximum possible lift in an unseparated incompressible flow. First, an airfoil velocity distribution is defined and optimized using boundary-layer theory and the calculus of variations. The resulting velocity distribution is then used as an input for an inverse airfoil design program which provides the corresponding airfoil shape. Since there is no guarantee that an arbitrarily defined velocity distribution will yield a physically possible airfoil shape, some parametric adjustments in the optimized distributions are required in order to obtain realistic and practical airfoil geometries. Wind-tunnel tests of two different airfoils (one assuming a laminar rooftop and the other a turbulent rooftop) have been conducted and in both cases the results met the theoretically predicted performance; for example, the laminar section exhibited a low drag range of $C_D \simeq 0.0085$ from $C_L = 0.8$ to $C_L = 2.2$.

Nomenclature

a, b = integration constants, see Eq. (8)
c = airfoil chord
C_L = lift coefficient = $L/(1/2)\rho V^2 c$
C_p = pressure coefficient = $(p - p_\infty)(1/2)\rho V_\infty{}^2$
C_p = pressure coefficient defined by Eq. (6)
p = static pressure
Re_∞ = freestream Reynolds number based on airfoil chord = $V_\infty c/\nu$
$Re_{s\infty}$ = Reynolds number defined by Eq. (12)
$Re_{\sigma 0}$ = Reynolds number defined by Eq. (6)
s = arc length along airfoil surface
s_p = location of leading-edge stagnation point
V_∞ = freestream velocity
v = local velocity on airfoil surface
$\bar{v}_b, \bar{v}_t$ = defined by Eqs. (3) and (4)
x = distance along chord line
Γ = circulation about the airfoil
ν = kinematic viscosity
ρ = density
σ = independent variable for Stratford equations
σ_0 = reference length for Stratford relations
$(\ )_\infty$ = freestream conditions
$(\ )_{te}$ = conditions at the airfoil trailing edge
$(\ )_0$ = conditions at velocity peak on airfoil upper surface

Introduction

IT is desired to solve the problem in answer to the question: "What is the maximum lift coefficient which can be obtained from a monoelement airfoil, and what is the shape of that airfoil?" This question is clearly quite general, and it is necessary to qualify it to an extent that an engineering problem can be formulated and solved. Most airfoils are partially separated when they reach their absolute maximum lift coefficient, and their continued operation under such conditions is usually considered impractical. Moreover, the development of techniques for the analysis of separated flow has not reached a level of precision and reliability where meaningful and realistic optimization techniques can be applied. Thus, it seems reasonable, at least initially, to consider the problem of the design of a monoelement airfoil which provides the maximum lift in an unseparated flow.

Another important consideration in the design of a high-lift airfoil is the effect of compressibility. It is well known that, even though an airfoil may be operating at a low flight speed, the super velocities on its upper surface can be quite high—particularly at high lift coefficients. However, for the purposes of the present analysis, the flow is assumed to be incompressible.

The basic approach for the design of a maximum lift monoelement airfoil will be to first specify a velocity distribution and then calculate the corresponding airfoil shape. The velocity distribution must satisfy the three criteria: 1) the boundary layer does not separate; 2) the corresponding airfoil shape is practical and realistic; and 3) maximum possible C_L is obtained. This may be interpreted as a form of variational problem where an extremum of C_L is sought subject to the constraints imposed by 1 and 2 above. In this study, such a variational problem is formulated and solved using existing boundary-layer and potential-flow analyses.

This problem was first studied in Ref. 1 where a linearized solution was obtained. The approach used was to express the lift coefficient in terms of $\int C_p dx$ where the freestream was aligned with the x-axis. An optimized form for the pressure distribution $C_p(x)$ was obtained using boundary-layer theory and the calculus of variations, and Weber's second-order inverse airfoil method[4] was used to obtain the corresponding airfoil shape. The resulting solution airfoils were highly cambered and in some cases quite thick. This suggested that the problem should be studied using an exact nonlinear airfoil theory together with a more precise formulation of an optimized pressure distribution, which is the subject of the present study.

The problem of accurately designing an airfoil which corresponds to a specified velocity distribution should not be based on x as an independent variable since this implies that the airfoil shape is already known. Therefore, in this analysis the velocity distribution is specified as a function of s, the distance along the airfoil surface, where s begins at the lower surface trailing edge and runs clockwise around the airfoil surface to the upper surface trailing edge as shown in Fig. 1. This form of input is ideal from the standpoint of an accurate application of boundary-layer theory since s is is the natural choice for an independent variable.

The lift coefficient is readily expressed in terms of the

Presented as Paper 73-86 at the AIAA 11th Aerospace Sciences Meeting, Washington, D.C., January 10–12, 1973; submitted January 30, 1973; revision received May 23, 1973. This work was performed under the Douglas Aircraft Company Independent Research and Development Program. Patent Pending.

Index category: Aircraft Aerodynamics.

*Senior Engineer/Scientist, Aerodynamics Research Group. Member AIAA.

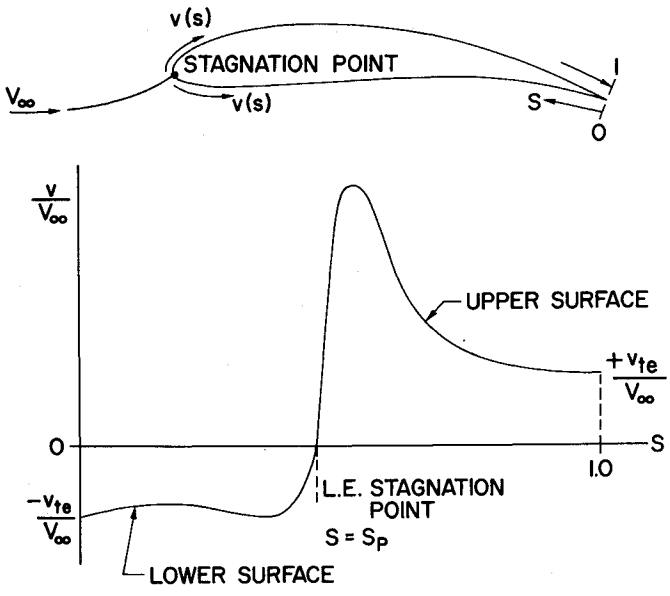

Fig. 1 General form of airfoil velocity distribution.

circulation about the airfoil, and the optimization problem becomes that of finding the velocity distribution $v(s)$ which maximizes

$$C_L = \frac{L}{1/2\,\rho V_\infty^2 c} = \frac{2\Gamma}{V_\infty c} = 2\oint \frac{v(s)}{V_\infty}\frac{ds}{c} \qquad (1)$$

subject to the constraints that the boundary layer does not separate and the corresponding airfoil profile closes and is not reentrant. As in the linearized problem, the approach is to first obtain a set of optimum velocity distributions using boundary-layer theory and the calculus of variations, and then adjust these distributions to obtain realistic and practical airfoil shapes.

Once the theoretical design is complete, an experimental evaluation is necessary to verify the airfoil's performance. Two airfoils, representing two basic design cases have been tested in the McDonnell Douglas low-speed wind tunnel at St. Louis, and their performance is presented following the development of the theory.

A similar theoretical approach has been used by Ormsbee and Chen in Ref. 2; however, the performance of one of their designs in a wind-tunnel test[3] did not reach their theoretical predictions. A possible explanation for this is offered in the conclusions of this paper.

Theoretical Development

General Form of Airfoil Velocity Distribution

The optimization of the velocity distribution for maximum lift is initially considered to be constrained by boundary-layer separation; however, certain basic airfoil geometry factors must be included. Referring to Fig. 1, the velocity distribution must have a leading edge stagnation point and it must also satisfy the Kutta condition at the trailing edge. Two possibilities exist at the trailing edge as far as the potential flow solution is concerned: if the trailing edge has a nonzero angle, the velocity must go to zero there; while if the trailing edge angle is zero, i.e., a cusp, the upper and lower surface velocities assume a value slightly less than freestream at the trailing edge. However, once the boundary layer is added, the flow outside the boundary layer passes the trailing edge with a continuous nonzero velocity. Therefore, the initial velocity distributions formulated will assume that the trailing edge is to be cusped. Finite trailing edge angles can easily

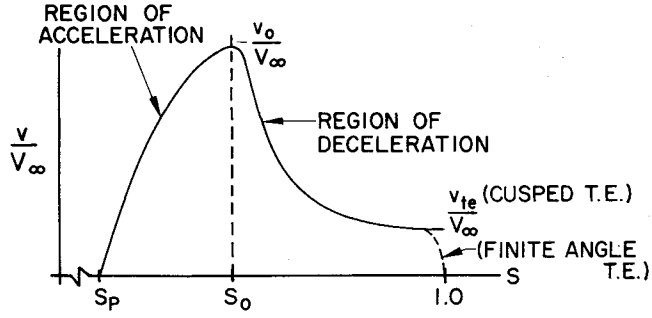

Fig. 2 General form of upper surface velocity distribution.

be prescribed once the initial solutions are obtained and understood.

Again referring to Fig. 1, the notation and sign convention to be used in this analysis can be explained. The velocity distribution on the airfoil surface is specified as a function of s, and the airfoil is taken as having a total perimeter of unity. Since the flow direction is the opposite of the direction of increasing s on the lower surface, the velocity there is always negative which is consistent with the definition of C_L as given by Eq. (1).

Expanding Eq. (1) to separate upper and lower surface flows gives

$$C_L = \frac{2}{c}\int_0^{s_p} \frac{v}{V_\infty} ds + \frac{2}{c}\int_{s_p}^{1} \frac{v}{V_\infty} ds \qquad (2)$$

where $s = s_p$ is the leading edge stagnation point and c is the airfoil chord. Considered as a variational problem, C_L can be written as the functional

$$C_L = C_L\left[\frac{v(s)}{V_\infty}; s_p, c\right]$$

That is, it is desired to find the distribution $v(s)/V_\infty$, $(0 \leq s \leq 1)$, the stagnation point location s_p, and the chord c which maximizes C_L. $v(s)/V_\infty$, s_p, and c cannot be chosen independently since they are implicitly connected according to standard airfoil theory.

It will prove convenient to rewrite Eq. (2) in the form

$$C_L = (2/c)[(\bar{v}_b/V_\infty s_p) + (\bar{v}_t/V_\infty)(1 - s_p)]$$

where $\bar{v}_b$ and $\bar{v}_t$ represent the average velocities on the bottom and top of the airfoil, respectively, i.e.,

$$\frac{\bar{v}_b}{V_\infty} = \frac{1}{s_p}\int_0^{s_p} \frac{v}{V_\infty} ds \qquad (3)$$

$$\frac{\bar{v}_t}{V_\infty} = \frac{1}{1 - s_p}\int_{s_p}^{1} \frac{v}{V_\infty} ds \qquad (4)$$

$\bar{v}_b/V_\infty$ will always be negative and it will detract from the total lift coefficient, and therefore $v(s)$ on the lower surface must be kept as small as possible; and this distribution, together with the optimum value for s_p, will be left open for the moment. The analysis will concentrate on obtaining an upper surface $v(s)$ distribution which maximizes $\bar{v}_t/V_\infty$ subject to the constraint that the boundary layer does not separate.

Boundary-Layer Analysis

The upper surface velocity distribution is taken to have the form shown in Fig. 2, namely a region of acceleration from the stagnation point s_p to the maximum velocity v_0, followed by a deceleration region to v_{te}. Rewriting Eq. (4)

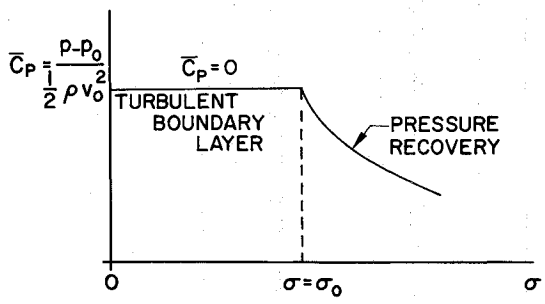

Fig. 3 Canonical pressure distribution of Stratford.[5]

in terms of the pressure coefficient gives

$$\frac{\bar{v}_t}{V_\infty} = \frac{1}{1-s_p}\int_{s_p}^{1}(1-C_p)^{1/2}ds \tag{5}$$

where the deceleration region is also called the pressure recovery region.

In order to shape the pressure recovery region, it is necessary to have a method for testing for boundary-layer separation. Stratford[5] does this and provides a basis for the analytical determination of the pressure recovery region which gives a distribution which just avoids separation along its entire length. Stratford's theory is derived for the canonical pressure distribution shown in Fig. 3 which consists of a constant pressure region for a distance σ_0 followed by a region of pressure recovery that begins at $\sigma = \sigma_0$ and continues downstream. The boundary layer is taken as turbulent over the entire region. Referring to Fig. 3, a pressure coefficient and Reynolds number are defined by

$$\bar{C}_p = (p-p_0)/{}^{1}/_{2}\rho v_0^2 \text{ and } Re_{\sigma 0} = v_0\sigma_0/\nu \tag{6}$$

where p_0 and v_0 are the static pressure and velocity along the constant pressure region. Stratford's solution is given by the relations

$$\bar{C}_p\left(\frac{\sigma}{\sigma_0}\right) = 0.49\left\{(Re_{\sigma 0})^{1/5}\left[\left(\frac{\sigma}{\sigma_0}\right)^{1/5}-1\right]\right\}^{1/3}, \quad \bar{C}_p \le 4/7 \tag{7}$$

$$\bar{C}_p\left(\frac{\sigma}{\sigma_0}\right) = 1 - \frac{a}{[(\sigma/\sigma_0)+b]^{1/2}}; \quad \bar{C}_p \ge 4/7 \tag{8}$$

Equations (7) and (8) represent a pressure recovery distribution for which boundary-layer separation is imminent but does not occur over the entire length of the pressure recovery region. The constants a and b in Eq. (8) are chosen to match $\bar{C}_p$ and $d\bar{C}_p/d\sigma$ when $\bar{C}_p = 4/7$. Stratford[6] has experimentally checked a flow whose pressure distribution is given by Eqs. (7) and (8), and found that it did not separate and exhibited a "good margin of stability."

The airfoil problem considered in this study requires that the flow originates from stagnation at $s = s_p$, and the velocity monotonically increases to $v = v_0$ at $s = s_0$ as indicated in Fig. 2. Stratford has provided two integral relations to account for this so that Eqs. (7) and (8) which are based on the velocity distribution of Fig. 3 may be applied to the airfoil problem. These integral relations are derived from the requirement that the boundary-layer momentum thickness for the case of a laminar acceleration region, the case of a turbulent acceleration region, and the constant velocity region of Fig. 3 be the same at the beginning of the deceleration region for all three cases. For a turbulent boundary-layer acceleration region this yields approximately

$$\sigma_0 = \int_{s_p}^{s_0}\left(\frac{v}{v_0}\right)^3 ds \tag{9}$$

and for a laminar boundary-layer acceleration region it gives

$$\sigma_0 = 38.2(Re_{\sigma 0})^{-3/8}\left[\int_{s_p}^{s_0}\left(\frac{v}{v_0}\right)^5 d\left(\frac{s}{s_0-s_p}\right)\right]^{-5/8}(s_0-s_p) \tag{10}$$

In effect, Eqs. (9) and (10) provide a lengthening of the distance from $s = s_p$ to $s = s_0$ over the distance from $\sigma = 0$ to $\sigma = \sigma_0$ when an acceleration region exists as opposed to a constant velocity region (Fig. 4). s represents the actual distance along the airfoil surface, and σ represents a distance from an origin which is located at a distance σ_0 behind the velocity peak on the upper surface of the airfoil. This lengthening is a consequence of the fact that a boundary layer, either laminar or turbulent, thickens more slowly in an accelerating flow than in a region of constant velocity, and a laminar boundary layer thickens more slowly than a turbulent boundary layer when both experience the same velocity distribution. A combination of Eqs. (9) and (10) applies when transition occurs at some intermediate point of the region upstream σ_0.

Using their respective definitions, C_p can be expressed in terms of $\bar{C}_p$ as

$$C_p = (v_0/V_\infty)^2(\bar{C}_p - 1) + 1$$

and conditions at the trailing edge give

$$(v_0/V_\infty)^2 = (1-C_{pte})/(1-\bar{C}_{pte}) \tag{11}$$

where $\bar{C}_{pte} = \bar{C}_p[(\sigma/\sigma_0)_{te}]$ as given by Eqs. (7) and (8). Thus, Eq. (11) provides a simple relation between the length of the recovery region, $(\sigma/\sigma_0)_{te}$; the magnitude of the pressure peak, $\bar{C}_{pmin} = 1 - (v_0/V_\infty)^2$; and the trailing edge pressure, C_{pte}, for the Stratford imminent separation pressure recovery distribution. The Reynolds number $Re_{\sigma 0}$ used in Eq. (7) is related to a more conventional form (Fig. 1)

$$Re_{s\infty} = 2V_\infty(1-s_p)/\nu \tag{12}$$

by using Eq. (11) to obtain

$$Re_{\sigma 0} = \{[1-C_{pte}]/[1-\bar{C}_{pte}]\}^{1/2}[\sigma_0/(1-s_p)]Re_{s\infty} \tag{13}$$

It is noted that the distance $1 - s_p$ will be only slightly greater than the airfoil chord, and therefore $Re_{s\infty}$ will be

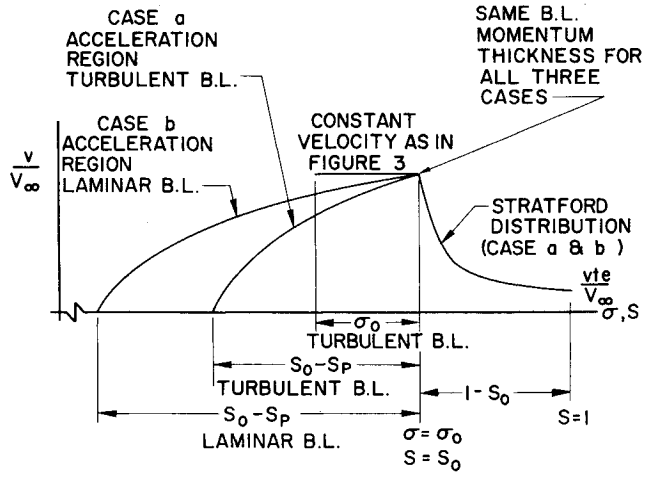

Fig. 4 Upper surface velocity distribution with a Stratford recovery region.

effectively equivalent to the conventional freestream Reynolds number, $Re_\infty = V_\infty c/\nu$.

Formulation and Optimization of Upper Surface Velocity Distribution

The analysis of Stratford provides a pressure distribution which recovers a given pressure difference in the shortest possible distance without separation; and, therefore, for the purpose of maximizing the lift, it appears logical to employ such a distribution for pressure recovery on the upper surface of the airfoil. Two cases will be considered. Case a: A turbulent boundary layer exists over the entire upper surface of the airfoil. Case b: A laminar boundary layer exists from the leading stagnation point s_p to the maximum velocity point s_0, with instantaneous transition to a turbulent boundary layer at s_0.

The form for the upper surface velocity distribution for both cases is shown in Fig. 4. This amounts to an arbitrary acceleration region from $s = s_p$ to $s = s_0$, followed by the Stratford deceleration region from $s = s_0$ to $s = 1$. From Eq. (4), $\bar{v}_t/V_\infty$ is given by

$$\frac{v_t}{V_\infty} = \frac{\int_{s_p}^{s_0} v/V_\infty \, ds + \int_{s_0}^{1} v/V_\infty \, ds}{1 - s_p} \tag{14}$$

and the problem is to maximize $\bar{v}_t/V_\infty$ while satisfying Eq. (9) for case a, and Eq. (10) for case b. The parameters Re_{σ_0} and v_{te}/V_∞ are left free at this point; and, since a Stratford deceleration distribution has been assumed, the second integral term of Eq. (14) is known as a function of Re_{σ_0} and v_{te}/V_∞, i.e.,

$$\int_{s_0}^{1} \frac{v}{V_\infty} ds = I\left[\left(\frac{\sigma}{\sigma_0}\right)_{te}, \frac{v_{te}}{V_\infty}, Re_{\sigma 0}\right] \tag{15}$$

where I is the same function for cases a and b. The parameter $(\sigma/\sigma_0)_{te}$ represents the length of the pressure recovery region and it is related to the magnitude of the pressure recovery by Eq. (11).

Referring to Fig. 4, it can be seen that the normalizing distance $1 - s_p$ can be considered as a function of two things: first, the form of the acceleration velocity distribution which determines the distance $s_0 - s_p$ according to Eqs. (9) or (10); and, second, the magnitude of the pressure recovery which determines the distance $1 - s_0$ according to Eq. (11). Consequently, although it might at first appear that $\bar{v}_t/V_\infty$ would be maximized by the furthest possible extent of an accelerating velocity distribution, the dependence of the normalizing distance $1 - s_p$ on the acceleration distribution precludes such an assumption.

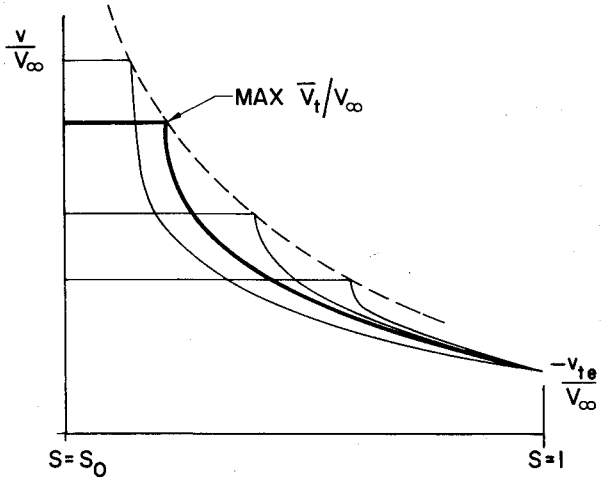

Fig. 5 Family of nonseparating flat rooftop velocity distributions. $Re_{\sigma 0}$ and v_{te}/V_∞ are fixed (not to scale).

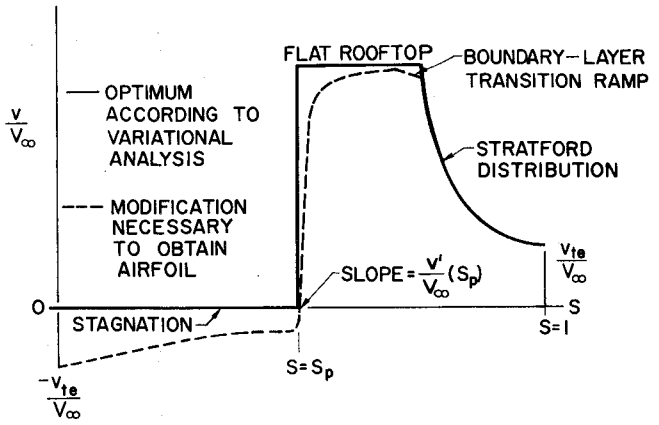

Fig. 6 Optimized form of airfoil velocity distribution including modification necessary for obtaining an airfoil shape.

In order to maximize $\bar{v}_t/V_\infty$, a variational problem is considered where it is sought to determine the form of the accelerating velocity distribution $v(s)/V_\infty$, $s_p \leq s \leq s_0$, and the value of the parameter $(\sigma/\sigma_0)_{te}$ which provide the desired extremum. The two parameters v_{te}/V_∞ and Re_{σ_0} are left free: v_{te}/V_∞ will be needed to adjust the velocity distribution to obtain a realistic airfoil shape, and Re_{σ_0} will be specified by Eq. (13) to obtain the desired freestream Reynolds number Re_∞.

Applying the calculus of variations yields the basic solution that a flat rooftop velocity (or pressure) distribution maximizes $\bar{v}_t/V_\infty$ for both cases a and b. There exists an infinite family of such flat rooftop distributions for a fixed set of the parameter v_{te}/V_∞ and Re_{σ_0}, and the variational solution also specifies that value of $(\sigma/\sigma_0)_{te}$ which defines the particular member of the family which maximizes $\bar{v}_t/V_\infty$ (Fig. 5). It should be noted that, for a fixed set of the parameters v_{te}/V_∞ and Re_{σ_0}, the resulting optimum velocity distribution for case b (laminar rooftop) will have a longer and higher rooftop region than for case a (turbulent rooftop).

Final Form for Optimized Velocity Distribution

The analysis of the previous section has indicated that C_L will be maximized by using an airfoil velocity distribution of the form shown in Fig. 6 by the solid line. This distribution is made of: $v(s)/V_\infty = 0$ over the entire lower surface, $v(s)/V_\infty$ given by a flat rooftop plus Stratford distribution on the upper surface, and s_p specified as small as possibly. Unfortunately, this distribution will not yield a meaningful airfoil shape due to the discontinuities present and the fact that true stagnation can only occur at a single point near the leading edge. Therefore, the velocity distribution has been modified as shown by the broken lines in Fig. 6.

The slope $v'(s_p)$ (Fig. 6) is used to control the resulting airfoil's leading edge radius, and the remaining portion of the upper surface acceleration region is shaped to provide good off-design performance ($\alpha > \alpha_{design}$) and still remain as close as possible to the limiting flat rooftop. A short boundary-layer transition ramp at the corner of the rooftop region is used for case b, and this is also included for case a to ease the boundary layer's introduction to the severe initial Stratford gradient. Since this modification to the upper surface velocity distribution results in a rooftop which is no longer flat, the length and height of the new

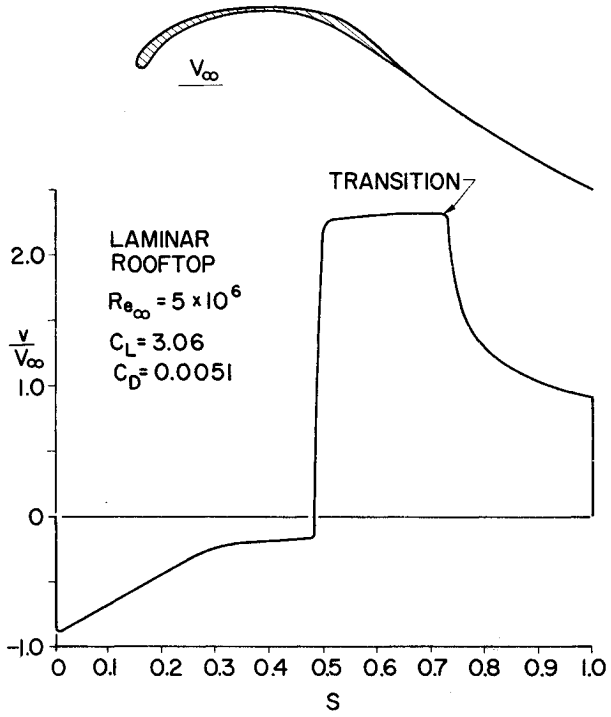

Fig. 7 Airfoil design and velocity distribution neglecting practical considerations.

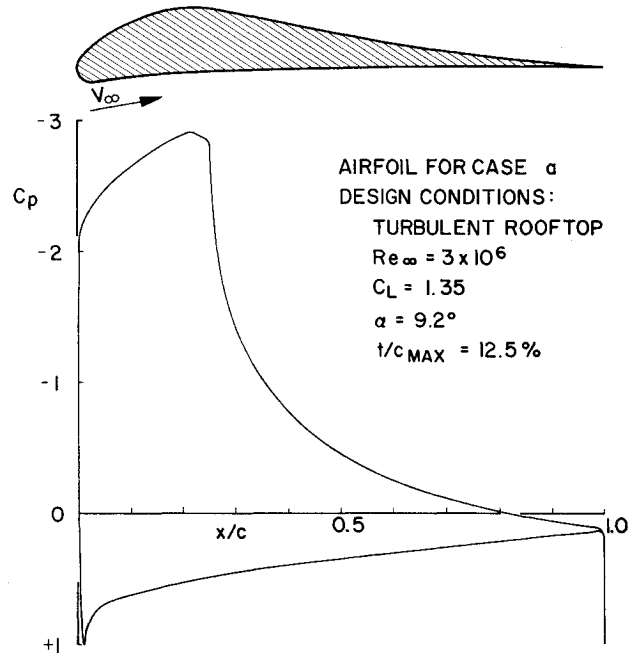

Fig. 9 Airfoil design and theoretical pressure distribution for wind tunnel test, case a.

rooftop could be increased, in principle, according to Eqs. (9) and (10). However, for the distribution considered in this study, this correction would be small, and it is felt that by neglecting it the resulting velocity distributions will be a bit more conservative.

The lower surface distribution is modified subject to two general constraints: first, that the velocity remains as low as possible in the interest of obtaining the maximum possible lift; and, second, that the flow continuously accelerates from the leading edge stagnation point to the trailing edge velocity v_{te}/V_∞ in the interest of minimizing the drag. In addition, the distribution near the stagnation point is shaped to provide good off-design performance at lift coefficients below the design value ($\alpha < \alpha_{design}$).

The resulting modified velocity distributions can no longer be called optimum (in a purely mathematical sense). For lack of a better word, they will be referred to as "optimized velocity distributions" with the understanding that this qualification exists.

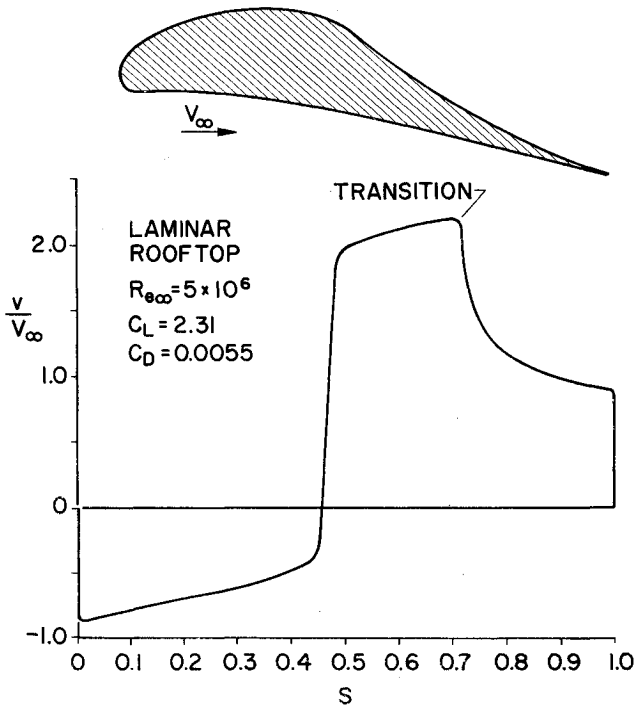

Fig. 8 Airfoil design and velocity distribution with practical thickness and leading edge geometry.

Inverse Airfoil Solution

Once a desired optimized airfoil velocity distribution has been developed, it remains to determine the corresponding airfoil shape. James[7] has developed a powerful inverse airfoil design program which provides exact solutions for the airfoil design problem. This program uses as input the airfoil velocity distribution as a function of s as shown in Fig. 1. It is well known that an arbitrarily prescribed velocity distribution is not likely to provide a corresponding closed and nonreentrant airfoil shape. The James program modifies the input velocity distribution to ensure that the modified distribution provides a closed (but not necessarily nonreentrant) airfoil shape. The modified velocity distribution may be considered the closest allowable distribution—in a least squares sense—to the input velocity distribution. By comparing the input and resulting modified (output) velocity distribution, the input distribution is easily adjusted (by varying v_{te}/V_∞, s_p, the level of the lower surface velocity distribution, etc.) so that agreement between the input and output distributions is obtained.

In addition to the velocity distribution, the James program requires that the desired airfoil trailing edge angle also be input explicitly. This, in principle, amounts to an overspecified problem since the velocity distribution itself implicitly defines the trailing edge angle. However, in reality, it is not practical to expect that an input velocity distribution will contain enough detail in the last two percent of the chord to provide an accurate definition of the trailing edge angle. Since the input distribution will be modified to provide a closed airfoil as described above,

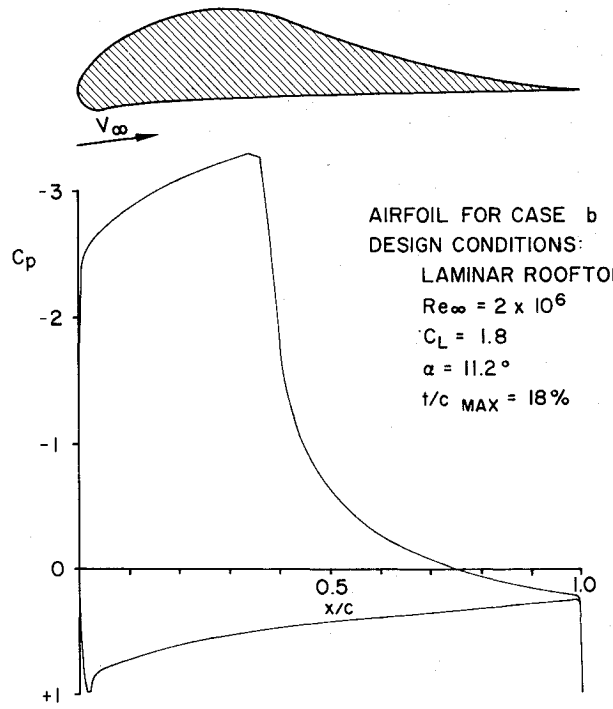

Fig. 10 Airfoil design and theoretical pressure distribution for wind tunnel test, case b.

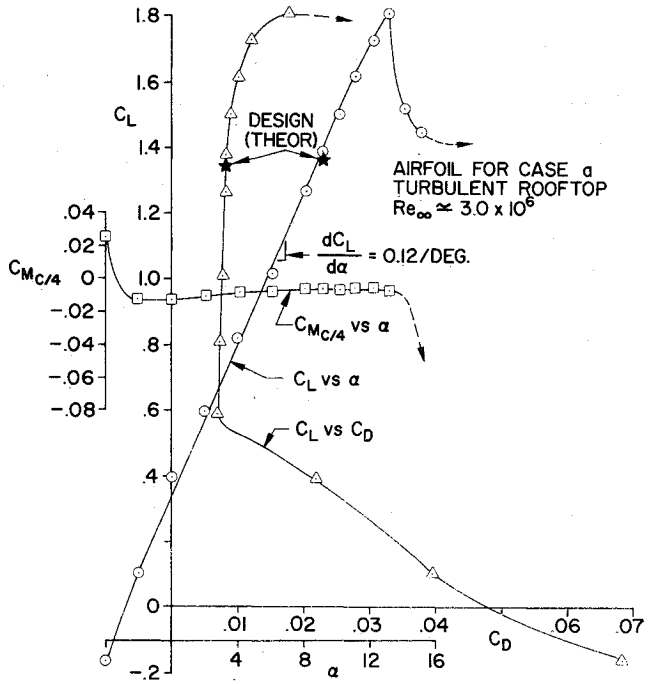

Fig. 11 Experimental lift curve and drag polar, turbulent rooftop airfoil, case a. Test conducted at $Re_\infty = 3 \times 10^6$.

the minor adjustment of the velocity distribution near the trailing edge which is required in order to obtain a specified trailing edge angle becomes insignificant as long as the specified angle is not too large.

Theoretical Design Results

Stated in their simplest form, the requirements on the airfoil geometry are that it is nonreentrant and that it has a rounded leading edge and sharp trailing edge. According to the variational analysis, for maximum lift it is desirable to obtain an airfoil velocity distribution which is as close as possible to that indicated by the solid line in Fig. 6. By strictly following this approach, the airfoil shape and corresponding velocity distribution of Fig. 7 was obtained for case b with a freestream Reynolds number of five million. This result may be regarded as significant from a purely theoretical point of view: it implies that the maximum lift coefficient which can be obtained from a monoelement airfoil in an unseparated incompressible flow at a Reynolds number of five million is about 3.0.

From a practical standpoint, the airfoil of Fig. 7 does not appear to be very useful. Its sharp leading edge will tend to cause separation when the airfoil is operated at angles of attack other than the design value, and it is probably too thin as far as structural considerations are concerned. Consequently, a sample airfoil design has been computed where a reduction in the value of the lift coefficient has been accepted in order to obtain reasonable performance over an angle of attack range together with an airfoil shape which is structurally feasible, and this result is shown in Fig. 8.

Experimental Evaluation

Two airfoils were prepared for testing: the airfoil shown in Fig. 9 was designed for a freestream Reynolds number of three million for case a, and the airfoil of Fig. 10 was designed for a freestream Reynolds number of two million for case b. The design pressure distributions were tested for separation using two independent theoretical boundary-layer calculation programs: the Douglas turbulent boundary-layer program,[8] and the NASA-Lewis boundary-layer program.[9] Neither program predicted separation over the entire pressure recovery region on either airfoil. For the airfoil of case b (Fig. 10), it was found that if transition were located upstream of the peak pressure

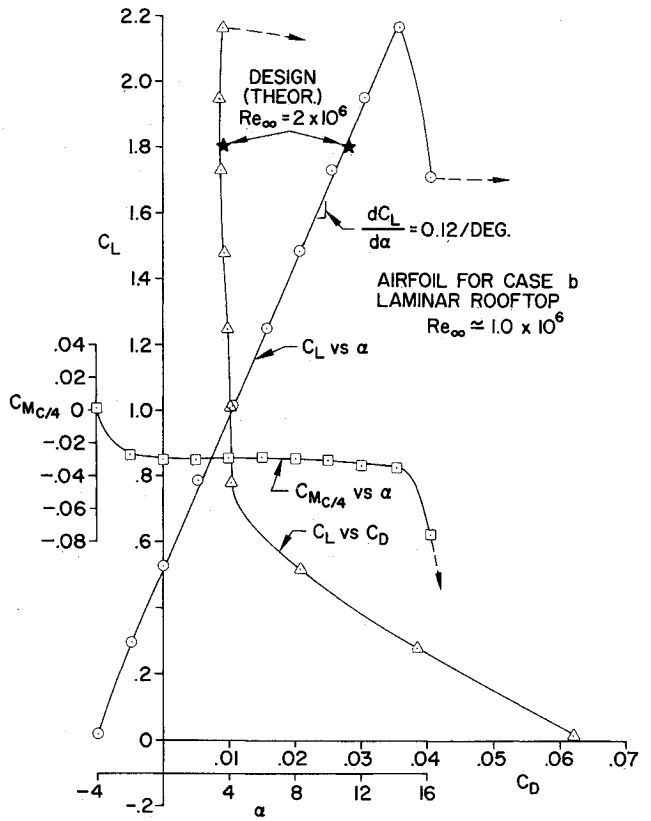

Fig. 12 Experimental lift curve and drag polar, laminar rooftop airfoil, case b. Test conducted at $Re_\infty = 1 \times 10^6$.

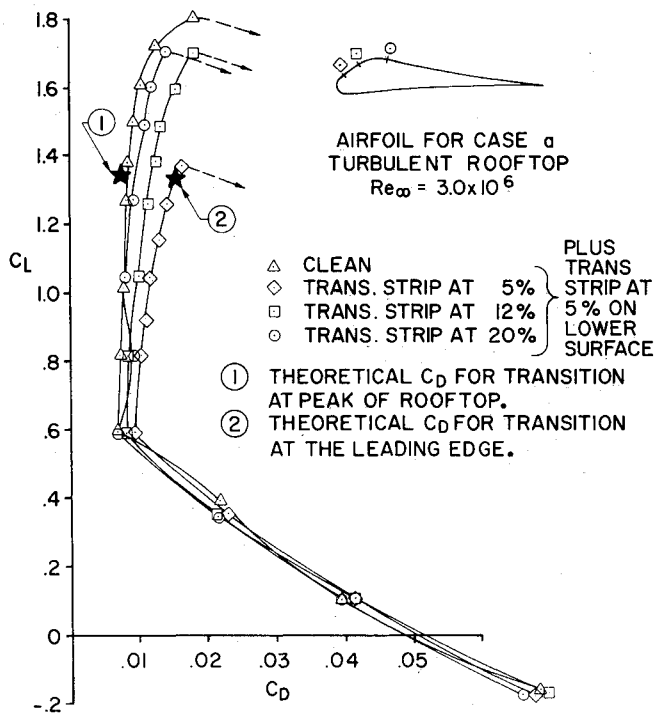

Fig. 13 Experimental drag polars showing the effect of transition strips, turbulent rooftop airfoil, case a.

point on the airfoil's upper surface, both the Douglas and NASA boundary-layer programs predicted separation somewhere along the Stratford pressure recovery distribution. The airfoil of case a (Fig. 9) remained fully attached even when transition was assumed to occur at the leading edge.

The results from the boundary-layer programs were used to calculate theoretical drag coefficients for the airfoils. Assuming transition at the leading edge for the airfoil of case a gave $C_D \simeq 0.017$, while assuming a laminar boundary layer over the entire lower surface and up to the rooftop peak on the upper surface gave $C_D = 0.0075$. For the airfoil of case b (which requires a laminar rooftop), the theoretically calculated drag was $C_D \simeq 0.0085$, where a laminary boundary layer was assumed over the entire lower surface. Boundary-layer displacement thickness calculations for both airfoils indicated a reduction in the lift coefficient of $\Delta C_L = -0.04$ at the design condition.

The experimental evaluation of the airfoils was conducted in the McDonnell Douglas 8.5 × 12-foot Low Speed Wind Tunnel in St. Louis with inserts used to obtain a 2-foot wide × 8.5-foot high two-dimensional test channel. Models of 27-in. chord with both spanwise and chordwise pressure taps were used. The tests were conducted at freestream Reynolds numbers from one to three million; and pressure, wake, and balance data were recorded. In addition, flow visualization studies were carried out using yarn tufts to check on flow separation, and china clay to identify boundary-layer transition.

The results of the wind-tunnel tests are given in Figs. 11–14. Figures 11 and 12 are the drag polars along with the corresponding C_L vs α and $C_{mc/4}$ vs α curves for the airfoils of case a and case b, respectively. It was necessary to conduct most of the testing of the airfoil for case b (laminar rooftop) at $Re_\infty = 10^6$ because freestream turbulence in the tunnel test section caused premature transition on the rooftop region when the tunnel was operated at higher Reynolds numbers. This was verified using china clay. Tunnel turbulence did not significantly affect the performance of the airfoil for case a which worked about equally well at Reynolds numbers from one to three million.

Figure 13 shows the effect of transition strips placed at various locations on the rooftop region for the airfoil of case a. Also shown are the theoretically predicted values of C_D for the two extremes: laminar flow over the rooftop region and the lower surface, and turbulent flow over the entire airfoil. (The early stall for the most forward transition strip location is partially attributed to the strip being too thick.) For the airfoil of case b, the addition of a transition strip on the rooftop region near the leading edge reduced the airfoil's $C_{L\max}$ to about 1.0.

A family of theoretical and experimental chordwise pressure distributions is given in Fig. 14 for the airfoil of case a. The theoretical distributions are based on the potential flow calculation of Ref. 10 without any correction for boundary-layer thickness. These results indicate that the flow remained attached all the way to the trailing edge. A laminar separation bubble appears on the lower surface near the leading edge at $\alpha = 0°$, and this accounts for the drag rise below $C_L = 0.6$ (Fig. 11).

The mechanism of the stalling of the airfoils was observed using yarn tufts located over the entire upper surface pressure recovery region. Both airfoils exhibited the same behavior in that the flow remained completely attached until the stalling angle was reached at which point the entire recovery region separated instantaneously. Reducing the angle of attack less than one half a degree resulted in an instantaneous and complete reattachment indicating almost a total lack of hysteresis effect on stall recovery.

Conclusions

One of the more important results of this study is that it has demonstrated the ability to define and solve a variational problem in optimal incompressible airfoil design. Moreover, the experimental results indicate an almost total verification of the theoretical predictions. That such a problem can be solved and experimentally verified re-

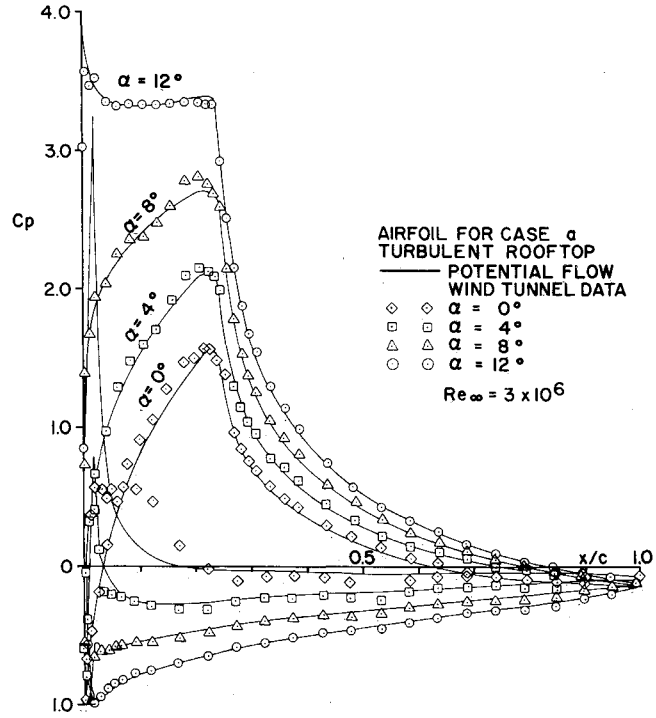

Fig. 14 Potential flow and experimental pressure distributions, turbulent rooftop airfoil, case a.

flects quite favorably on the current stage of boundary-layer and potential-flow theory.

The airfoil designs may be considered exact in that they correspond precisely to the optimized velocity distributions, and the boundary-layer analysis has been applied along the airfoil surface rather than using the distance along the chord line. However, no particular airfoil solution is unique as may be seen from Figs. 7 and 8.

Some of the more significant results of the two wind-tunnel tests include the following. 1) Both airfoils exceeded their design lift coefficients by a comfortable margin, and they exhibited a very wide C_L-range where the drag was almost constant and quite low. 2) The pitching moment coefficients for both airfoils are quite low. 3) The airfoils appeared to be surprisingly independent of Reynolds number in the range of one to three million. (This assumes the absence of the tunnel turbulence effects.) 4) The flow over the pressure recovery region appeared to be very stable and remained completely attached until stall occurred. 5) The agreement between the theoretical potential flow and experimental pressure distributions (and lift coefficients) implies that the airfoils experience little deterioration in performance due to boundary-layer thickness effects.

The results of the wind-tunnel test[3] of a high lift airfoil designed by Ormsbee and Chen[2] show that the experimental lift curve slope was less than the theoretically predicted value (which included boundary-layer thickness effects), and the airfoil stalled before it reached its design angle of attack. No drag data is given. Some of this difficulty is explained by the fact that boundary-layer separation occurred on the tunnel walls at high lift coefficients; however, it appears that the airfoil design itself is also responsible for some of the problems encountered.

More specifically, the optimized velocity distribution as prescribed by Ormsbee and Chen is characterized as having a rather large velocity difference immediately upstream of the trailing edge (i.e., $v_{te}/V_\infty = 1$ on the upper surface and $v_{te}/V_\infty \simeq 0.85$ on the lower surface). At the trailing edge, both upper and lower surface velocities drop to stagnation which results in an airfoil with a nonzero trailing edge angle, and the large velocity difference immediately upstream produces a relatively thick trailing edge with a large trailing edge angle. It would appear that this form of trailing edge geometry encourages a more severe local flow separation there which results in a modified Kutta condition and a consequent decrease in the lift curve slope. In addition, this condition can only serve to deteriorate the airfoil's $C_{L\max}$ performance and increase its drag, particularly for an airfoil with a Stratford imminent separation pressure recovery distribution.

The choice of a high value for v_{te}/V_∞ on the upper surface is desirable from the standpoint of increasing the lift which may be carried (i.e., in the present analysis, $\bar{v}_t/V_\infty$ increases with increasing v_{te}/V_∞), but the value of this parameter is limited by the consideration of obtaining an acceptable airfoil geometry at the trailing edge. In the present study, it has been found that values of v_{te}/V_∞ between 0.8 and 0.95 (on both upper and lower surfaces) provide a trailing edge geometry which virtually eliminates any tendency for local separation there, and this is reflected in the experimental results.

Finally, the results of this study appear to substantiate the viability of the Stratford imminent separation pressure recovery distribution. As a useful device in the design of high-performance airfoil sections, it would appear that these distributions are indeed practical and reliable. In most applications, it would probably be best to predicate the design on the assumption of a turbulent rather than a laminar rooftop.

References

[1]Liebeck, R. H. and Ormsbee, A. I., "Optimization of Airfoils for Maximum Lift," *Journal of Aircraft,* Vol. 7, No. 5, Sept.–Oct. 1970, pp. 409–415.

[2]Ormsbee, A. I. and Chen, A. W., "Multiple Element Airfoils Optimized for Maximum Lift Coefficient," *AIAA Journal,* Vol. 10, No. 12, Dec. 1972, pp. 1620–1624.

[3]Bingham, G. J. and Chen, A. W., "Low-Speed Aerodynamic Characteristics of an Airfoil Optimized for Maximum Lift Coefficient," TN D-7071, Dec. 1972, NASA.

[4]Weber, J., "The Calculation of the Pressure Distribution on the Surface of Thick Cambered Wings and Design of Wings with Given Pressure Distribution," R&M 3026, June 1955, Aeronautical Research Council, London, England.

[5]Stratford, B. S., "The Prediction of Separation of the Turbulent Boundary Layer," *Journal of Fluid Mechanics,* Vol. 5, 1959, pp. 1–16.

[6]Stratford, B. S., "An Experimental Flow with Zero Skin Friction Throughout its Region of Pressure Rise," *Journal of Fluid Mechanics,* Vol. 5, 1959, pp. 17–35.

[7]James, R. M., "A New Look at Two-Dimensional Incompressible Airfoil Theory," Rept. MDC-J0918/01, May 1971, Douglas Aircraft Co., Long Beach, Calif.

[8]Cebeci, T., Smith, A.M.O., and Wang, L. C., "A Finite-Difference Method for Calculating Compressible Laminar and Turbulent Boundary Layers," Rept. DAC 67131, Pt. I, March 1969, Douglas Aircraft Co., Long Beach, Calif.

[9]McNalley W. D., "FORTRAN Program for Calculating Compressible Laminar and Turbulent Boundary Layers in Arbitrary Pressure Gradients," TN D-5681, May 1970, NASA.

[10]Hess, J. L. and Smith, A. M. O., "Calculation of Potential Flow about Arbitrary Bodies," *Progress in Aeronautical Sciences,* edited by D. Kuchemann, Vol. 8, Pergamon Press, New York, 1966.